Geochemical constraints on mantle sources for volcanic rocks from Mt. Melbourne and the western Ross Sea, Antarctica

Mi Jung Lee*[1], (mjlee@kopri.re.kr), Jong Ik Lee[1], Taehoon Kim[1], and Keisuke Nagao[1]

[1]Division of Polar Earth System Sciences, Korea Polar Research Institute (KOPRI), Incheon 406-840, Korea

ABSTRACT

We report geochemical and isotope data (Sr, Nd, Pb) of submarine samples from the Terror Rift Region and subaerial lavas from Mt. Melbourne Volcanic Field (MMVF) in the western Ross Sea. The MMVF samples can be subdivided into Groups A and B based on their temporal and spatial distribution. All samples are alkaline, ranging from basanite to trachybasalt, and exhibit an HIMU-like isotopic signature ($^{206}Pb/^{204}Pb$ = 18.510–19.683, $^{87}Sr/^{86}Sr$ = 0.70300–0.70398, $^{143}Nd/^{144}Nd$ = 0.51284–0.51297) and trace element affinities (Ce/Pb = 25–35, Nb/U = 45–60, Ba/Nb = 5–13, La/Nb = 0.5–0.9). The Terror Rift submarine lavas (0.46–0.57 Ma) display a distinct trend, with more primitive geochemical characteristics (higher MgO (7.2–9.8 wt.%) and CaO (9.9–11.9 wt%) and stronger HIMU signature than those of MMVF basalts. Results from a rare earth element (REE) model suggest that the Terror Rift submarine lavas are derived from small degrees (1–2%) of partial melting of an amphibole-bearing garnet peridotite mantle source. Incompatible trace element ratios (e.g., Ba/Nb = 6.4–13.2, La/YbN = 14.4–23.2, Dy/Yb = 2.2–3.0) and isotopic compositions of the MMVF Group A and B volcanics suggest derivation from higher degrees (2–5%) of partial melting of a garnet peridotite source and strong influence of an EMI-type mantle source. The stronger HIMU signature of the Terror Rift submarine lavas appears to be related to smaller degrees of partial melting, suggesting preferential sampling of the HIMU component in the less partially melted rocks from the Cenozoic NVL magmatism. In contrast, the higher degree of MMVF A and B magmas can be explained by greater interaction with heterogeneous lithospheric mantle, resulting in a diluted HIMU signature compared with that of the Terror Rift submarine lavas.

Regional & sample location map

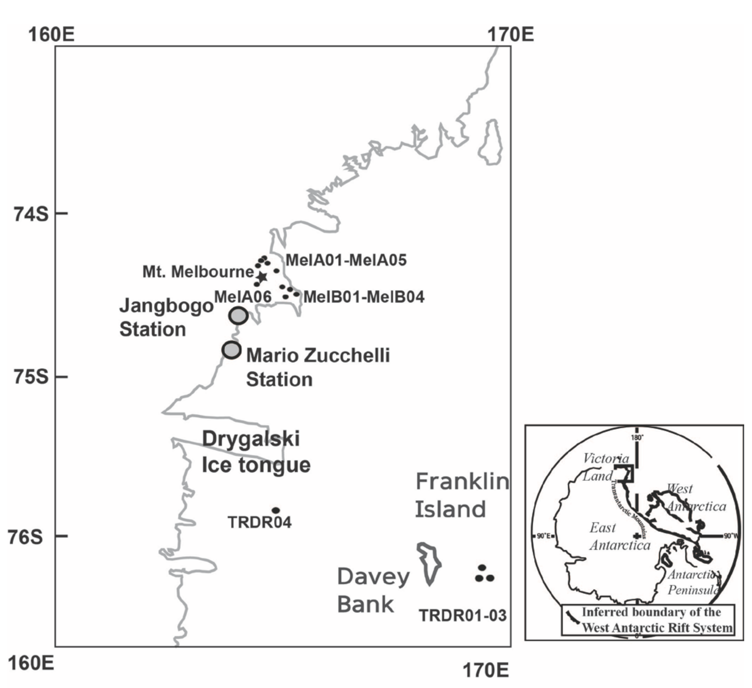

Fig. 1. Regional location map of the Northern Victoria Land and sampling sites.

K/Ar ages

Table 1. Results of K-Ar dating for volcanic lavas from Victoria Lad Basin and Mt. Melbourne Volcanic Field.

Sample	Sampling site: Latitude	Sampling site: Longitude	K (wt.%)	Weight molten (g)	^{36}Ar (10^{-10} cm^3/g)	$^{40}Ar/^{36}Ar$	Rad. ^{40}Ar (10^{-8} cm^3/g)	K-Ar age (Ma)	Air-fraction (%)
MELA01	74 13.932 S	164 43.002 E	1.49	0.3578	18.11 ± 0.91	306.48 ± 0.59	1.90 ± 0.14	0.33 ± 0.03	96.58
MELA01	74 13.932 S	164 43.002 E	1.49	0.1161	16.27 ± 0.82	305.81 ± 0.71	1.60 ± 0.14	0.28 ± 0.03	96.79
MELA04	74 13.917 S	164 44.002 E	1.23	0.3907	7.16 ± 0.36	309.67 ± 0.64	0.98 ± 0.07	0.20 ± 0.01	95.59
MELA04	74 13.917 S	164 44.002 E	1.23	0.1561	6.71 ± 0.35	310.57 ± 0.62	0.98 ± 0.07	0.20 ± 0.01	95.31
MELA06	74 20.970 S	164 41.423 E	1.43	0.3504	13.09 ± 0.66	299.4 ± 0.58	0.40 ± 0.08	0.07 ± 0.01	98.86
MELA06	74 20.970 S	164 41.423 E	1.43	0.1247	12.99 ± 0.66	301.08 ± 0.66	0.66 ± 0.09	0.12 ± 0.02	98.31
MELB01	74 29.195 S	165 17.383 E	1.65	0.3424	4.00 ± 0.20	496.68 ± 2.21	8.03 ± 0.42	1.25 ± 0.09	59.60
MELB02	74 29.195 S	165 17.383 E	1.61	0.4124	8.28 ± 0.42	397.04 ± 0.95	8.36 ± 0.43	1.34 ± 0.07	74.55
MELB03	74 29.195 S	165 17.383 E	1.64	0.3059	10.21 ± 0.52	377.89 ± 1.10	8.36 ± 0.43	1.31 ± 0.09	78.33
MELB04	74 29.195 S	165 17.382 E	1.66	0.362	7.96 ± 0.40	403.37 ± 1.47	8.54 ± 0.44	1.32 ± 0.07	73.38
TRDR02	76 6.256 S	169 12.675 E	1.65	0.3862	18.23 ± 0.91	307.68 ± 0.69	2.13 ± 0.16	0.33 ± 0.03	96.20
TRDR02	76 6.256 S	169 12.675 E	1.65	0.1148	17.15 ± 0.87	306.83 ± 0.71	1.86 ± 0.15	0.29 ± 0.03	96.47
TRDR03	76 6.256 S	169 12.675 E	1.61	0.3242	22.60 ± 1.13	311.72 ± 0.82	3.55 ± 0.25	0.57 ± 0.05	94.96
TRDR03	76 6.256 S	169 12.675 E	1.61	0.0893	21.53 ± 1.09	309.45 ± 0.66	2.90 ± 0.20	0.46 ± 0.04	95.65
TRDR04	75 57.282 S	165 39.145 E	1.82	0.3519	17.61 ± 0.88	314.27 ± 0.69	3.22 ± 0.20	0.46 ± 0.03	94.19
TRDR04	75 57.282 S	165 39.145 E	1.82	0.1257	17.48 ± 0.88	312.52 ± 0.61	2.89 ± 0.18	0.41 ± 0.03	94.71
Standard sample									
Baba tuff #c			6.56	0.0293	15.55 ± 0.89	2219.65 ± 61.5	299.08 ± 15.3	11.71 ± 0.64	13.34
Baba tuff #d			6.56	0.0366	14.85 ± 0.83	2456.40 ± 58.0	320.90 ± 16.8	12.56 ± 0.70	12.05
Baba tuff #120304a			6.56	0.0273	13.58 ± 0.82	2529.92 ± 87.8	303.47 ± 15.6	11.88 ± 0.65	11.70

Sr-Nd-Pb isotopic compositions

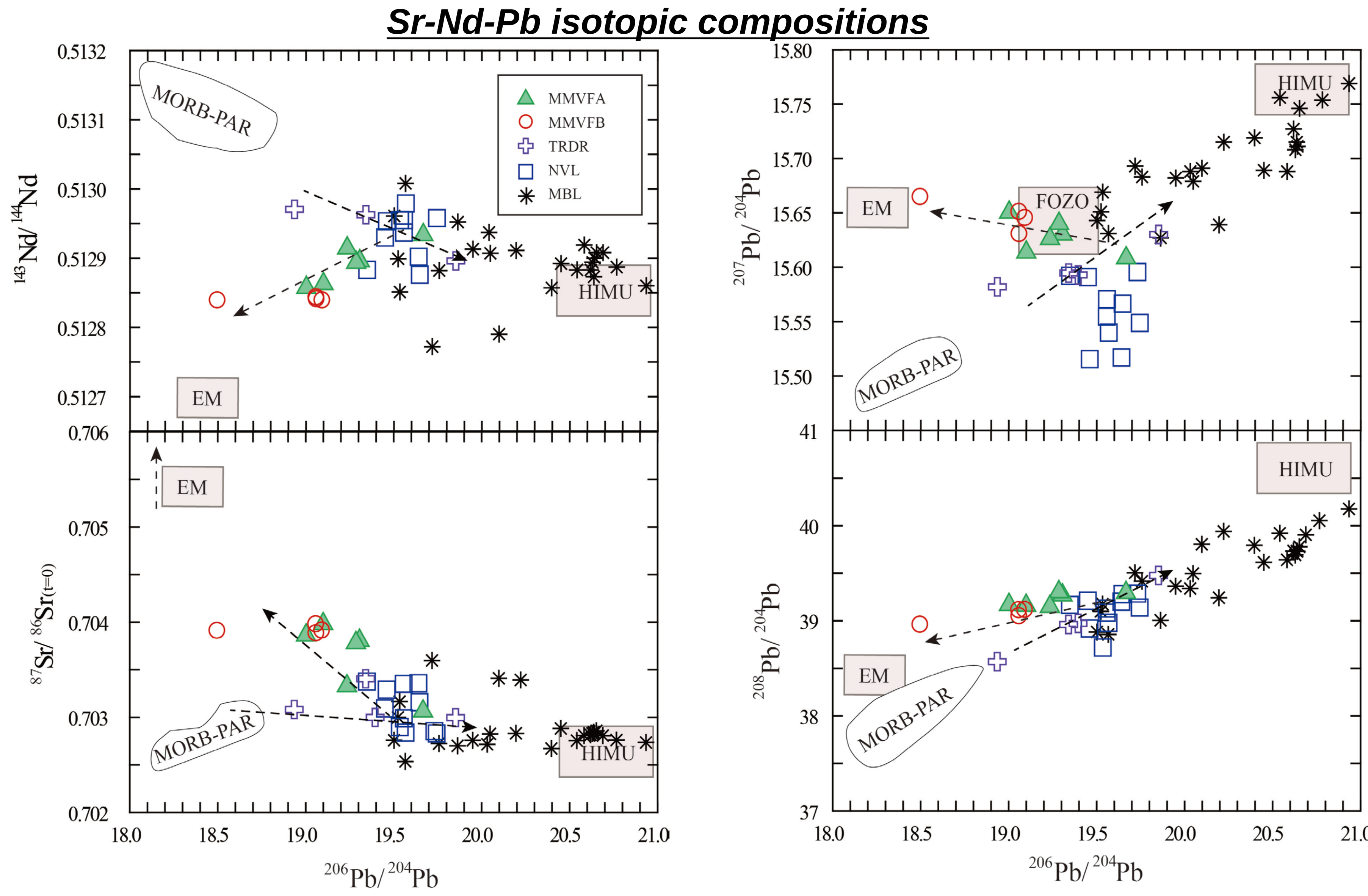

Fig. 4. Sr-Nd-Pb isotopic compositions for the MMVF basalts and Terror Rift submarine lavas from NVL, Antarctica. Data sources for NVL and MBL samples are the same as in Fig 3. MORB-PAR (Pacific Antarctic Ridge) are from Vlastelic et al. (1999). End-member mantle components are from Zindler and Hart (1986). The Sr-Nd-Pb isotope data of the Terror Rift submarine samples forms an array between the MORB and HIMU sources, indicating an involvement of a HIMU-like mantle component with the depleted MORB-like source to the magma generation. To explain isotopic compositions of the MMVF group A and B basalts, a third enriched component is required.

Major and trace element compositions

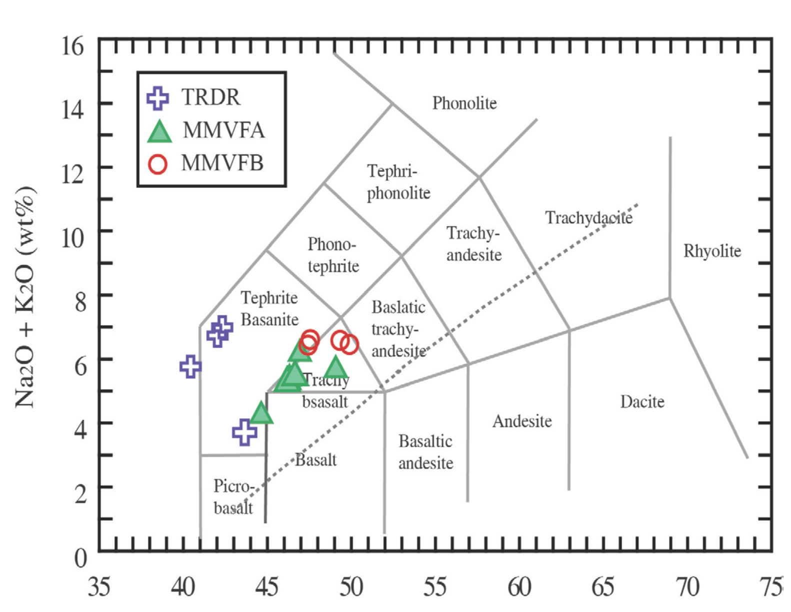

Fig. 2. Total alkalis vs. SiO_2 diagram for basalts from the Mt. Melbourne Volcanic Field and Terror Rift Region (the framework is after Le Bas et al., 1985). Abbreviations are: TRDR, Terror Rift Dredge basalts; MMVFA and MMVFB, Mt. Melbourne Volcanic Field group A and B basalts.

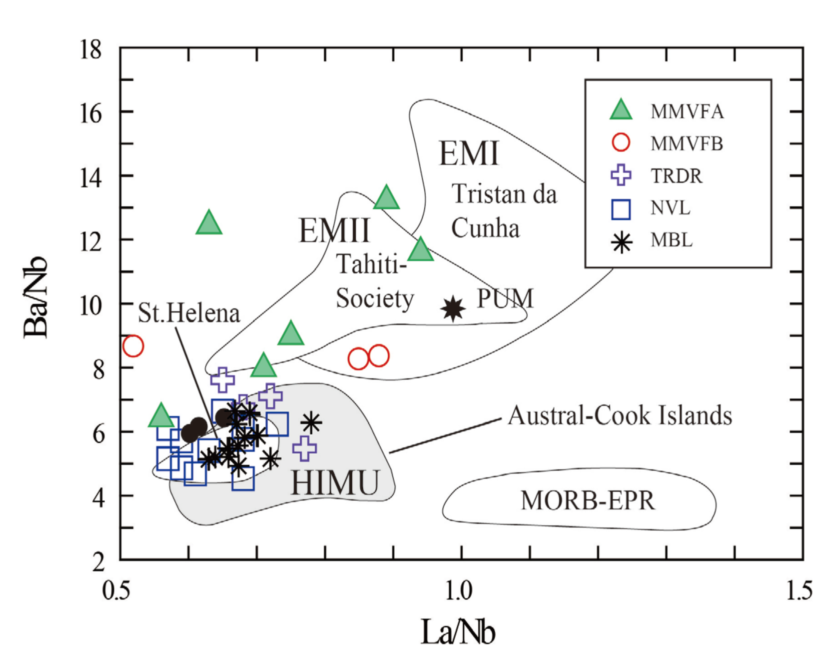

Fig. 3. Ba/Nb vs. La/Nb ratios. Data for McMurdo Volcanic Group basalts from the Northern Victoria Land (NVL, Nardini et al., 2009) and Marie Bird Land basalts (MBL, Panter et al., 2006) are displayed together for comparison. Data field for Austral-Cook Island, St. Helena basalts, which are known as representative HIMU-OIBs, Tristan da Cunha (EMI) and Tahiti-Society (EMII) are compiled from PETDB database (http://www.petdb.org/index.jsp). MORB-EPR (East Pacific Rise) are from the PETDB database (http://petdb.org/index.jpg). PMU, Primitive Upper Mantle (McDonough& Sun, 1995). Terror Rift submarine samples have lower Ba/La and La/Nb ratios than those of MMVF group A and B samples and are comparable with those of HIMU-like OIB.

Melting processes : REE modeling

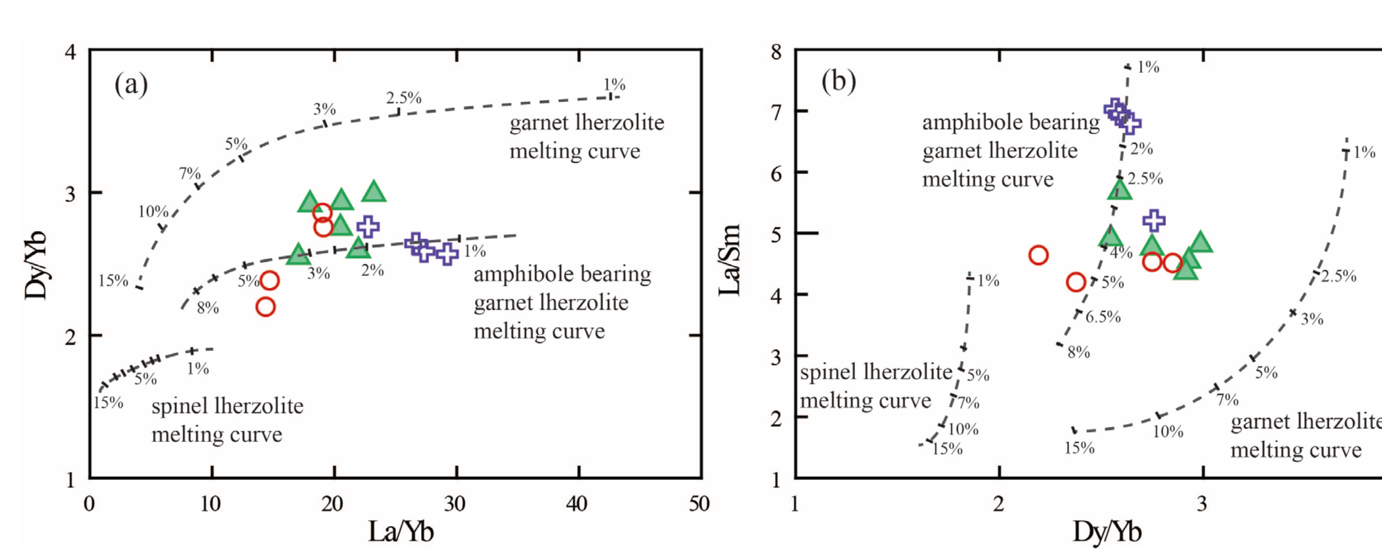

-Dy/Yb ratios of the melt from a hypothetical garnet lherzolite is too high.
-It is required a phase in the mantle source that show a greater compatibility for MREE than HREE (e.g. amphibole: D_{Dy}= 0.7; D_{yb}=0.59; Chazot et al (1996).
- Modeling an amphibole-bearing garnet lherzolite source produced a closer fit to the compositions of the Terror Rift samples in the Dy/Yb vs. La/Yb and La/Sm vs. Dy/Yb.
- The data for the Terror Rift samples are consistent with 1–2% melting of an amphibole-bearing garnet lherzolite source.
- The MMVF Group A and B samples generally show large variations in MREE composition, reflecting the heterogeneous characteristics of their source.
- The degree of partial melting of the MMVF Group A and B samples appears to be greater (about 2–5 %) than that of the Terror Rift submarine samples.

Fig. 5. Calculated partial melting curves assuming non-modal batch melting of spinel, garnet and amphibole-bearing garnet lherzolite. Phase proportions in solid and melt modes for a hypothetical spinel lherzolite used for model calculations are $ol_{0.578} + opx_{0.27} + cpx_{0.119} + sp_{0.033}$ and $ol_{0.1} + opx_{0.27} + cpx_{0.5} + sp_{0.13}$, and for a hypothetical garnet lherzolite $ol_{0.598} + opx_{0.211} + cpx_{0.115} + gt_{0.115}$ and $ol_{0.05} + opx_{0.20} + cpx_{0.30} + gt_{0.45}$, respectively. Phase proportions in solid and melt modes for a hypothetical amphibole-bearing garnet lherzolite are $ol_{0.514} + opx_{0.213} + cpx_{0.123} + gt_{0.075} + amp_{0.075}$ and $ol_{0.05} + opx_{0.18} + cpx_{0.205} + gt_{0.25} + amp_{0.315}$, respectively. Modeling used the REE distribution coefficients of McKenzie & O'Nions (1991) and Chazot *et al.* (1996). The spinel and garnet lherzolite mantle compositions are from Tang *et al.* (2006). The amphibole-bearing garnet lherzolite composition is from McCoy-West *et al.* (2010). Abbreviations: ol, olivine; opx, orthopyroxene; cpx, clinopyroxene; sp, spinel; gt, garnet; amp, amphibole.

Spider diagrams

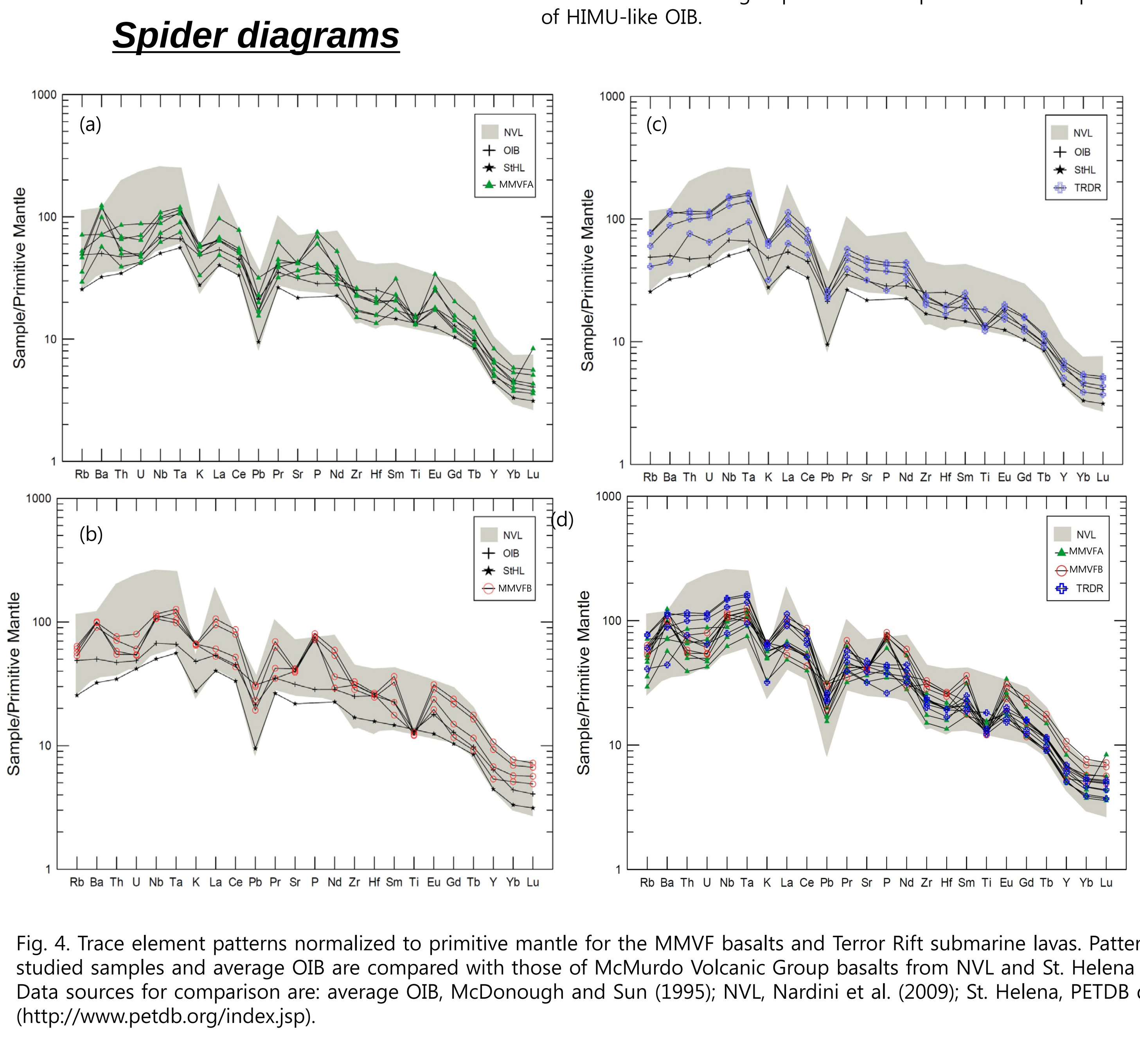

Fig. 4. Trace element patterns normalized to primitive mantle for the MMVF basalts and Terror Rift submarine lavas. Patterns of the studied samples and average OIB are compared with those of McMurdo Volcanic Group basalts from NVL and St. Helena HIMU-OIB. Data sources for comparison are: average OIB, McDonough and Sun (1995); NVL, Nardini et al. (2009); St. Helena, PETDB database (http://www.petdb.org/index.jsp).

Conclusions

1. The Terror Rift submarine and MMVF Group A and B samples are alkaline, ranging from basanite to trachybasalt, and show the OIB-like patterns of trace element distribution, with a prominent depletion in K and Pb. Compared with the MMVF Group A and B basalts, the Terror Rift submarine samples have lower SiO_2 and Al_2O_3, higher MgO and CaO, higher ratios of more to less incompatible elements (La/Yb, La/Sm, Nb/Y, Th/Yb, and U/Pb), and more radiogenic Pb and Nd and less radiogenic Sr isotopic compositions.

2. The K/Ar ages suggest that MMVF Group A and B and Terror Rift submarine lavas represent products of three distinct magmatic episodes. MMVF Group A samples shows the youngest ages, ranging from 0.1 to 0.3 Ma, Group B samples have the oldest ages, from 1.25 to 1.34 Ma, and the Terror Rift samples have ages of 0.46–0.57 Ma.

3. REE modeling and the isotopic compositions of the Terror Rift samples suggest that they were derived from low (1–2 %) partial melting of an amphibole-bearing garnet peridotite mantle source with preferential melting of a HIMU-like component in metasomatized lithospheric mantle. In contrast, the geochemical characteristics of the MMVF Group A and B basalts reflect the large geographic scale of sampling (higher degrees (2–5%) of melting) of heterogeneous lithospheric mantle and could be explained by the consequence of mixing and averaging of melts involving depleted MORB-like, HIMU-like, and EMI-like components.

4. We consider that edge-driven convective flow under the thinned lithospheric mantle of NVL toward the thick Antarctic Craton may have allowed upwelling of hot asthenospheric melts and triggered local melting of metasomatized veined lithospheric mantle.